

# Well Width Effects on Material Gain and Lasing Wavelength in InGaAsP / InP Nano-Heterostructure

Rashmi Yadav<sup>1</sup>, Pyare Lal<sup>1</sup>, F. Rahman<sup>2</sup>, S. Dalela<sup>3</sup>, P. A. Alvi<sup>1\*</sup>

<sup>1</sup>Department of Physics, Banasthali Vidyapith, Rajasthan (INDIA)

<sup>2</sup>Department of Physics, Aligarh Muslim University, Aligarh, UP (INDIA)

<sup>3</sup>Department of Pure and Applied Physics, University of Kota, Kota, Rajasthan (INDIA)

\*Corresponding author: drpaalvi@gmail.com

Received November 12, 2013; Revised January 09, 2014; Accepted January 20, 2014

**Abstract** This paper reports the effects of quantum well width on material gain and lasing wavelength of the InGaAsP / InP lasing nano-heterostructure which is based on simple SCH (Separate Confinement Heterostructure) design. The studies made in this paper are directed towards the well width dependent modeling of InGaAsP / InP lasing nano-heterostructure and simulation of the lasing characteristics such as material gain, differential gain, anti-guiding factor and refractive index change with carrier density. The outcomes of the work reported in this paper suggest that both the material gain and lasing wavelength can be controlled by varying width of the quantum well sandwiched between the barriers followed by claddings in the nano-structure. Since, the maximum material gain has been achieved at wavelength of 1.35  $\mu\text{m}$  for minimum quantum well width (2 nm) with in TE mode; therefore, InGaAsP / InP based nano-heterostructure with 2 nm well width may be very useful in the area of nano-optoelectronics.

**Keywords:** material gain, anti-guiding factor, InGaAsP, differential gain, carrier density

**Cite This Article:** Rashmi Yadav, Pyare Lal, F. Rahman, S. Dalela, and P. A. Alvi, "Well Width Effects on Material Gain and Lasing Wavelength in InGaAsP / InP Nano-Heterostructure." *Journal of Optoelectronics Engineering*, vol. 2, no. 1 (2014): 1-6. doi: 10.12691/joe-2-1-1.

## 1. Introduction

In the area of optoelectronics, recent developments have been directed towards quantum well (QW) based devices such as lasing heterostructures which offer the improved performance in the aspect of switching speed, long wavelength and high intense beam output. Quantum well (QW) lasing nano-heterostructure are seductive for research due to their physically and technology vital. For optical fiber communication systems, the semiconductor based nano-heterostructures emitting long wavelength (i.e. 1.3-1.55  $\mu\text{m}$ ) are considerable for technological weightage and this has led to theoretical and experiment work, specifically on the InGaAsP material system during the past few decades. InGaAsP / InP material system based multiple quantum well (MQW) lasing heterostructures are widely used in optical fiber communication system as light sources due to their interesting lasing wavelengths. In past few decades, for more semiconductors laser applications preferred the quantum well laser has been steadily grown until now. Recently, due to unusual properties of III-V semiconductors based quantum-size structures; they have drawn a very serious attention of researchers. Interestingly, formation of self-organized low-dimension semiconductor layers has drawn attention to the researchers due to the possibility of creating three-dimensional electron confinement in the uniform and

coherent (non-dislocation) clusters. In the present era, quantum size-lasing heterostructures are very significant sources for fiber optic communications and are key components of applications such as optical data storage and remote sensing [1,2]. In quantum well based lasing heterostructures, it is desirable to lower the threshold current before lasing begins, maximize optical gain and minimize the losses. Step based Separate Confinement Heterostructures (SCH) play a promising role in this context. In SCH based designs, the carriers get confined by heterostructure barriers so as to increase the carrier density in quantum well and therefore enhancing radiative recombination. As a result, a considerable amount of carriers is no more able to drift away to opposite electrode; they must recombine in the active region. The major benefits are continuous wave operation making them ideal for optoelectronic applications. Further advantages include less heat generation and less power consumption.

Recently, Wang Yang et al. fabricated 1.5  $\mu\text{m}$  InGaAsP / InP tunnel injection multiple quantum well Fabry Perrot (F-P) ridge laser, and investigated the cavity length dependence of temperature  $T_0$  [3]. InGaAsP quantum well active region generates good electrical confinement and large amount of gain leads to high quantum efficiency and low threshold current density [4]. By using the 4 x 4 Luttinger-Kohn Hamiltonian, the optical gain and valence effective masses in both types of quantum well (QW) lasers viz. InGaAlAs and InGaAsP under compressive strain have been calculated along with refractive index

change [5]. Carsten et al. presented that by varying the composition and changing the well thickness, the band gap of QWs can be engineered which is the major advantage [6]. Although, the lasing heterostructure based on material composition InGaAsP / InP have shown bad performance due to the small conduction band offset [7], even the heterostructure with well width of 2 nm (as in present work) has provided a maximum gain at the lasing wavelength of 1.35  $\mu\text{m}$  (wavelength of low attenuation).

The barrier strain effects of AlGaInAs-InP in MQWs at 1.3  $\mu\text{m}$ , well width dependence, threshold current density of GaAsSb / GaAs type-II quantum well (QW) lasers has been investigated [8,9]. However, the optical gain of lasing heterostructure is a mandatory parameter in characterizing the fabricated heterostructures and simulating their behavior. Recently, Lal et al. have simulated lasing characteristics along with material gain for AlGaAs / GaAs nano-heterostructure with in TE and TM mode [10]. This Structure was found suitable for the emission of NIR radiations. Beatrice et al studied theoretically well width dependence of gain and threshold current in AlGaAs based SCH (single quantum well) lasers [11]. In this paper, we have studied, extensively, the well width effect on the material gain and related lasing characteristics of InGaAsP / InP nano-heterostructure.

## 2. Structure Detail and Theory

The overall model of separate confinement nano-heterostructure (SCNH) of material composition  $\text{In}_{0.90}\text{Ga}_{0.10}\text{As}_{0.59}\text{P}_{0.41}$  / InP can be considered to consists of a single quantum well with thickness of 60  $\text{\AA}$  (quantum or active region) which contractive between two wide band gap layers of barrier (thickness 50  $\text{\AA}$ ) of InGaAsP material followed by cladding (thickness 100  $\text{\AA}$ ) of same material. The compositions of barriers and claddings are taken different in order to have different band gaps and refractive indices. The band gap of barriers is kept smaller than that of claddings while refractive index is larger for barriers and smaller for claddings. The overall nano-heterostructure is assumed to be grown on InP substrate pseudo morphically, as shown in Figure 1.

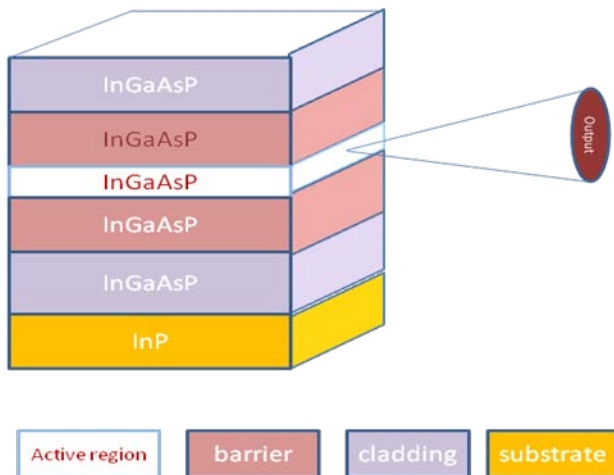


**Figure 1.** SCH based model for SQW nano-heterostructure of  $\text{In}_{0.90}\text{Ga}_{0.10}\text{As}_{0.59}\text{P}_{0.41}$  / InP

In our calculations, the conduction band dispersion profile is assumed to be parabolic. To calculate the

discrete energy levels within the semi parabolic conduction band, the single band effective mass equation can be used as [12];

$$-\frac{\hbar^2}{2m_c^*}\nabla^2\psi + V_c\psi = E_c\psi$$

Where  $\psi$  is envelope function,  $\hbar$  is reduced Plank's constant divided by  $2\pi$ ,  $m_c^*$  conduction effective mass,  $V_c$  potential of conduction band,  $E_c$  is conduction band electron energy level. For a strained quantum well, the conduction band potential is;

$$V_c = \begin{cases} \frac{2\delta_h}{3}, \text{Quantumwell} \\ \Delta V_{bc}, \text{Barrier} \\ \Delta V_{cc}, \text{Cladding} \end{cases}$$

where  $\delta_h$  is the hydrostatic potential and conduction band offsets of barrier and cladding layers are  $\Delta V_{bc}$  and  $\Delta V_{cc}$  respectively. The hydrostatic potential can be defined as;

$$\delta_h = 2a \left( 1 - \frac{C_{12}}{C_{11}} \right) \varepsilon$$

where  $\varepsilon$  is the strain constants of the barrier and quantum well layers that can be given as;

$$\varepsilon = (a_b - a_q) / a_b$$

where,  $a$  is the hydrostatic deformation potential,  $C_{11}$  and  $C_{12}$  are the elastic stiffness constants. For, non-parabolic valence band structure, the multiband effective mass theory can be used, that can give the coupled differential equations for heavy and light holes.

In order to evaluate envelope functions and the heavy and light hole energy bands, the Kohn-Luttinger Hamiltonian can be solved as follows;

$$\hat{H}\psi = \begin{bmatrix} H & M & N & 0 \\ M & L & 0 & N \\ N & 0 & L & -M \\ 0 & N & -M & H \end{bmatrix} \psi = E_v\psi$$

where

$$H = -\frac{\hbar^2}{2m_0} \left[ (k_x^2 + k_y^2)(\gamma_1 + \gamma_2) - (\gamma_1 - 2\gamma_2) \frac{\partial}{\partial z^2} \right] + V_{hh, lh}$$

$$L = -\frac{\hbar^2}{2m_0} \left[ k_x^2 + k_y^2 (\gamma_1 + \gamma_2) - (\gamma_1 + 2\gamma_2) \frac{\partial}{\partial z^2} \right] + V_{hh, lh}$$

$$M = \frac{i\sqrt{3}\hbar^2}{2m_0} (-k_y - ik_y) \gamma_3 \frac{\partial}{\partial z}$$

$$N = -i \frac{\sqrt{3}\hbar^2}{2m_0} \left[ \gamma_2 (k_x^2 + k_y^2) - 2i\gamma_3 k_x k_y \right]$$

where  $\psi$  is the envelope function, the energy eigen values in valence sub-bands for heavy and light hole is represented by  $E_v$ ,  $\hbar$  is the reduced plank constant divided by  $2\pi$ ,  $m_0$  is the mass of free electron,  $\gamma_1$ ,  $\gamma_2$  and  $\gamma_3$  are the Luttinger parameters,  $k_x$  and  $k_y$  are the transverse wave

vector components, the potential of valence sub-band for heavy hole is  $V_{hh}$ ,  $V_{lh}$  is the potential of the valence sub-band for light hole.

The heavy and light hole sub-band potential can be expressed as follows;

$$V_{hh} = \begin{cases} -\frac{1}{3}\delta_h + \delta_s, \text{Quantumwell} \\ -\Delta V_{bv}, \text{Barrier} \\ -\Delta V_{cv}, \text{Cladding} \end{cases}$$

$$V_{lh} = \begin{cases} -\frac{1}{3}\delta_h - \delta_s, \text{Quantumwell} \\ -\Delta V_{bv}, \text{Barrier} \\ -\Delta V_{cv}, \text{Cladding} \end{cases}$$

In the above expressions, the quantities  $\Delta V_{bv}$  and  $\Delta V_{cv}$  are valence band offsets for barriers and claddings, respectively. The quantity  $\delta_s$  represents the shear potential, can be expressed as follows;

$$\delta_s = 2b \left( 1 - \frac{2C_{12}}{C_{11}} \right) \varepsilon$$

where  $b$  is shear deformation potential.

The energy eigenvalues for a particle confined in the quantum well are given by;

$$E(n, k_x, k_y) = E_n + \frac{\hbar^2}{2m_n^*} (k_x^2 + k_y^2)$$

where  $E_n$  is the  $n$ th level confined-particle energy for carrier motion to the well,  $m_n^*$  is the effective mass for this level,  $k_x$ ,  $k_y$  are the wave vectors along  $x$  and  $y$  directions respectively.

Figure 2 describes the electrons and holes energy levels  $E_n$  confined in a quantum well.

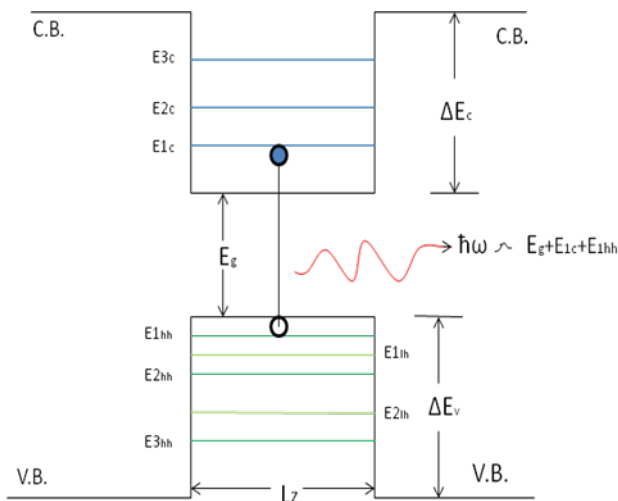


**Figure 2.** Schematic diagram of confined particle energy levels of electrons, heavy holes and light holes in QW

The energy levels for electrons, heavy holes, and light holes of confined Particle shown by  $E_{1c}$ ,  $E_{2c}$  and  $E_{3c}$ ,  $E_{1hh}$ ,  $E_{2hh}$ ,  $E_{3hh}$  and  $E_{1lh}$ ,  $E_{2lh}$ ,  $E_{3lh}$  respectively.

The optical gain as a function of the photon energy for quantum well structure can be written as;

$$G(E') = \frac{q^2 |M_B|^2}{E' \varepsilon_o m_o^2 c \hbar n_{eff} W} \sum_{i,j} \int_{E_g}^{E_{gb}} m_{r,ij} C_{ij} A_{ij} (f_c - f_v) L(E) dE$$

where

$q$ . electron charge.

$|M_B|^2$ . bulk momentum transition matrix element.

$\varepsilon_o$ . free space permittivity.

$C$ . speed of light in vacuum.

$n_{eff}$ . effective refractive index of the laser structure.

$W$ . width of the quantum well.

$i, j$ . conduction and valence band quantum numbers.

$m_{r,ij}$ . spatially weighted reduced mass for transition.

$C_{ij}$ . spatial overlap factor between the states  $i$  and  $j$ .

$A_{ij}$ . angular anisotropy factor.

$f_c$ ,  $f_v$ . electron quasi fermi function in the conduction and valence band.

$L(E)$ . Lorentzian lineshape function.

The Lorentzian line shape function can be defined as;

$$L(E) = \frac{1}{\pi} \frac{\hbar/\tau_{in}}{(E' - E)^2 + (\hbar/\tau_{in})^2}$$

where  $\tau_{in}$  is intra-band relaxation time.

In the equation of material gain,  $f_c$  and  $f_v$  are to be calculated. The quasi-Fermi levels  $E_{fc}$  and  $E_{fv}$  can be calculated by using the following equations;

$$N = \frac{m_n^* kT}{\pi \hbar^2 L_z} \sum_i \ln[1 + e^{(E_{fc} - E_i)/kT}]$$

$$P = \frac{m_{hh}^* kT}{\pi \hbar^2 L_z} \sum_i \ln[1 + e^{(E_{fv} - E_{hi})/kT}]$$

$$+ \frac{m_{lh}^* kT}{\pi \hbar^2 L_z} \sum_i \ln[1 + e^{(E_{fv} - E_{li})/kT}]$$

where

$N$  = electron concentration.

$P$  = hole concentration.

$m_n^*$  = effective mass of electron.

$m_{hh}^*$  = effective mass of heavy hole.

$m_{lh}^*$  = effective mass of light hole.

In the above equations,  $E_{fc}$ ,  $E_{fv}$  the quasi fermi levels can be solved with a given carrier concentration and known energy levels.

Next, a very important parameter is anti-guiding factor that plays a very crucial role in lasing heterostructure and can be defined as in terms of refractive index change and differential gain as;

$$\alpha = -\frac{4\pi n'}{\lambda G'}$$

where the quantities  $G'$  and  $n'$  are the differential gain and differential refractive index change respectively for the heterostructure.

### 3. Results and Discussion

Assuming parabolic nature of conduction band dispersion profile, the one dimensional Schrödinger equation has been solved to obtain energies of electrons in conduction band of quantum well of the compound material  $\text{In}_{0.90}\text{Ga}_{0.10}\text{As}_{0.59}\text{P}_{0.41}$  over InP substrate, as shown in Figure 3. The compositions of wells and barriers are selected in such a way so that they are lattice matched, but the substrate is chosen in such a way so that the quantum wells are compressively strained by an amount of 1.2%, hence for compressively strained quantum well structure, proper selection of substrate is very important. In literature, it has been reported that the compressively strained quantum well structure, TE polarization mode dominates. The Compressive conduction and valence bands dispersion profiles for  $\text{In}_{0.90}\text{Ga}_{0.10}\text{As}_{0.59}\text{P}_{0.41}$  quantum well at temperature 300 K and strain  $\sim 1.2\%$  are shown in Figure 3. In Figure 3, it is clear that apart from the band edge ( $k_x = 0$ ), the conduction band energy is found to increase with the wave vector. In the dispersion profiles, it can be seen that the energy separation between conduction band and valence HH (heavy hole) subbands is also increasing with increasing wave vector. Moreover, according to the valence band dispersion profiles, apart from the band edge, the energy separation between the LH and HH (heavy hole) subbands is decreasing but the energy of SO (split off hole) subbands with respect to LH and HH valence subbands is increasing along the wave vector. The SO hole subbands arise due to spin-orbit interactions.

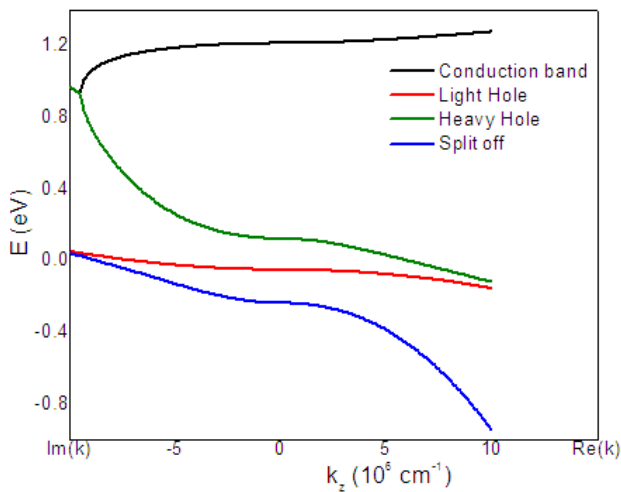


**Figure 3.** Compressive conduction and valence band dispersion profiles for  $\text{In}_{0.90}\text{Ga}_{0.10}\text{As}_{0.59}\text{P}_{0.41}$  quantum well at 300 K

In the study of material gain, the knowledge of behavior of quasi-Fermi level plays an important role. For the active layer of  $\text{In}_{0.90}\text{Ga}_{0.10}\text{As}_{0.59}\text{P}_{0.41}$  as a quantum well in the nano-heterostructure, the behavior of quasi-Fermi levels as a function of carrier densities in the conduction and valence bands have been shown in Figure 4. Basically, quasi-Fermi level is a new type of Fermi level that can describe the population density of each type of charge carriers (electrons and holes) in a semiconductor separately when their population density is displaced from the condition of equilibrium. Actually, the quasi-Fermi-levels of electrons and holes in the respective bands in a quantum well are calculated during photoluminescence under non-equilibrium condition [13]. The radiative behavior of opto-devices consisting of quantum wells

depends upon the quasi-Fermi level separation induced in the quantum well.

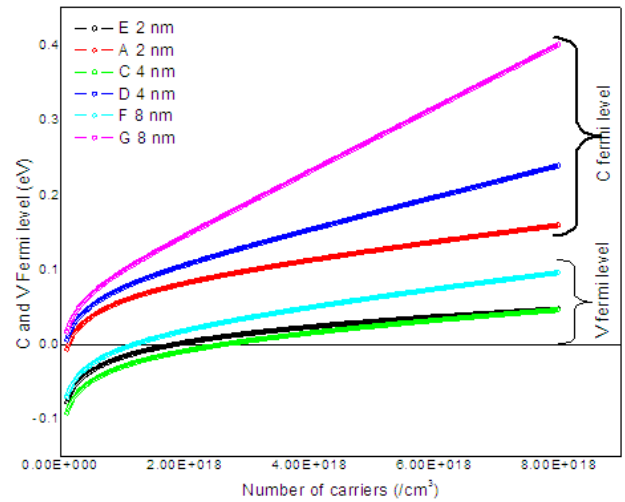


**Figure 4.** Behavior of quasi-Fermi levels in the conduction and valence bands

The study of refractive index spectrum of a quantum well in the nano-heterostructure is essential to the design and implementation of nano-opto-electronic devices. In case of heterostructure, the most important differences between the active region (quantum well) and barriers are generally in the energy bandgap and the refractive index. The differences in energy bandgap permit spatial confinement of injected carriers (electrons and holes), but the differences in refractive index can be used to form optical waveguides, therefore, in the heterostructure, it is important to know explicitly the refractive index variation with carrier density in the active or quantum region. In Figure 5, the refractive index change with carrier density in the quantum region of  $\text{In}_{0.90}\text{Ga}_{0.10}\text{As}_{0.59}\text{P}_{0.41}$  / InP nano-heterostructure has been shown. By studying the refractive index change of the active region in the nano-heterostructure and differential gain, the anti-guiding factor ( $\alpha$ -factor) can be estimated, which is a key parameter and responsible for optical or material gain associated with the nano-heterostructure. The anti-guiding factor determines the spectral width under both high speed direct modulation and continuous wave operation. However, it is essential to reduce the anti-guiding factor to reduce the spectral width. The range of anti-guiding factor for  $\text{In}_{0.71}\text{Ga}_{0.21}\text{Al}_{0.08}\text{As}$  / InP lasing nano-heterostructure having single quantum well at room temperature has been found to vary from 1.5 to 4 [14,15] and for AlGaAs / GaAs it has been reported to vary from 1.2 to 2.1 [10]. In Figure 6, the behavior of anti-guiding factor for  $\text{In}_{0.90}\text{Ga}_{0.10}\text{As}_{0.59}\text{P}_{0.41}$  / InP nano-heterostructure having single quantum well of different widths (2, 4, and 8 nm) have been shown. In Figure 6, it is clear that the range of anti-guiding factor is shifting towards higher values with increasing width of quantum well. For well width of 2 nm, it has been reported to vary from 1.0 to 1.1. This small range of anti-guiding factor is found suitable for the higher material gain and corresponding required wavelength for lasing action of the heterostructure. Moreover, it will be important to note that the anti-guiding factor plays the same role in order to exist the material gain in the waveguides, as the resistance does for existence of voltage gain in electric conductors. In case

of waveguides or heterostructure, a small or non-zero value is highly desirable for lasing applications because the higher values can lead to self-focusing, anti-guiding and beam filamentation. One thing should be clear that if the value of anti-guiding factor is decreased, the differential gain is increased.

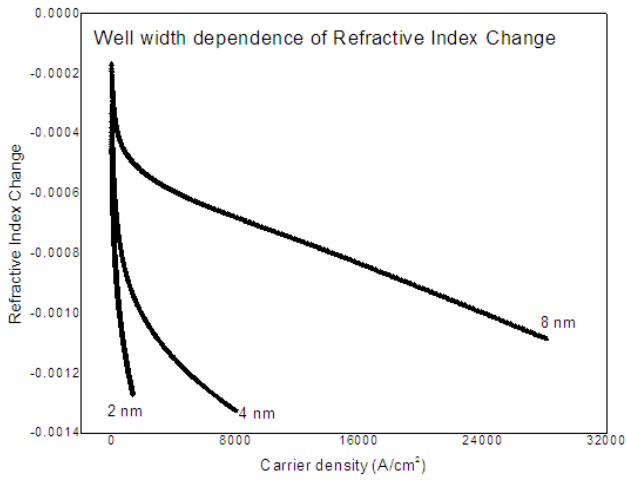


**Figure 5.** Well width dependence of refractive index change with carrier density

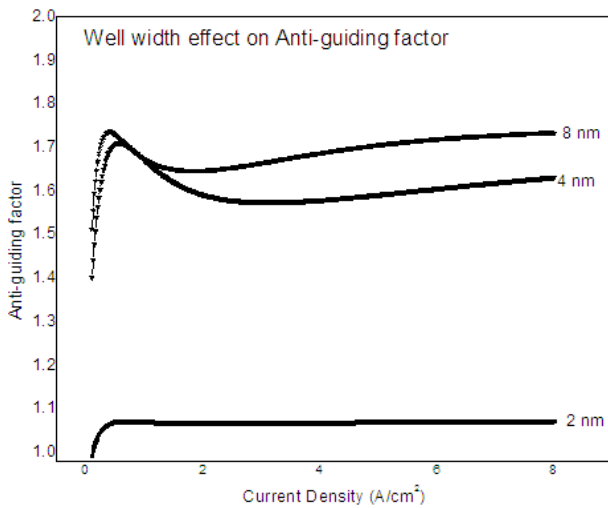


**Figure 6.** Well width effect on anti-guiding factor for InGaAsP / InP Nano-heterostructure

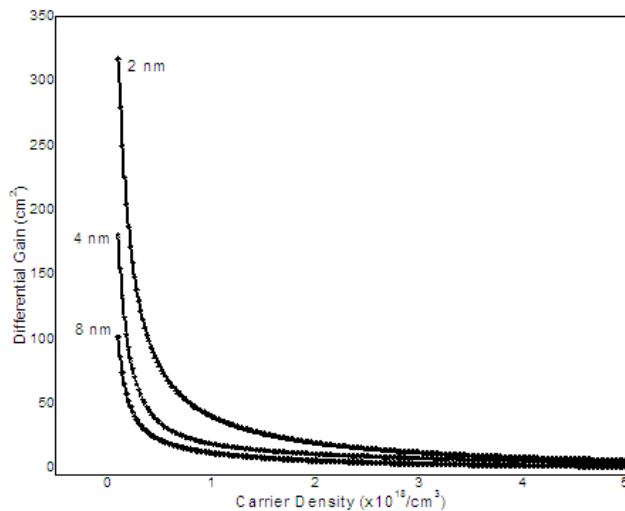


**Figure 7.** Behavior of differential gain at different well width of InGaAsP / InP Nano-heterostructure

The differential gain for  $\text{In}_{0.90}\text{Ga}_{0.10}\text{As}_{0.59}\text{P}_{0.41}$  / InP nano-heterostructure consisting of single quantum well has been calculated for different well widths (2, 4, and 8 nm) and plotted in Figure 7. In Figure 7, it is clear that the differential gain of the nano-heterostructure is decreasing with increase in carrier density, which is verified with the commonly observed fact that the differential gain of quantum well based lasing heterostructure decreases with increasing carrier density at higher injection current [16]. It may also be noted that on increasing width of the quantum well, the overall differential gain decreases which is due to the decrease in refractive index.

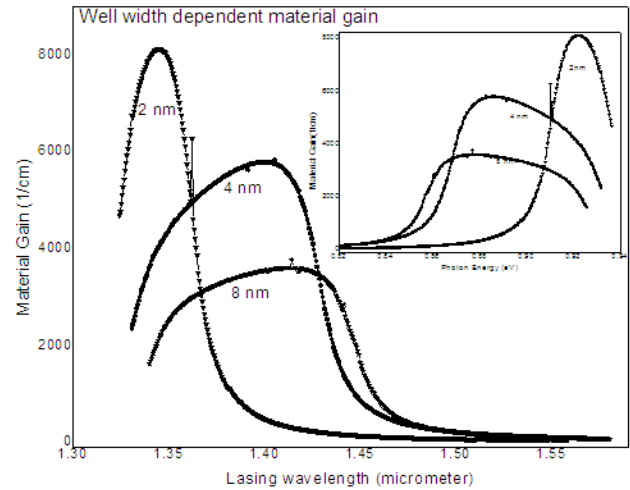


**Figure 8.** Well width dependence of material gain of InGaAsP / InP Nano-heterostructure

The well width dependence of gain spectra in terms of lasing wavelength have been studied and shown in Figure 8. In Figure 8, the TE mode gain spectra of  $\text{In}_{0.90}\text{Ga}_{0.10}\text{As}_{0.59}\text{P}_{0.41}$  / InP lasing nano-heterostructure having single quantum well of different widths (2, 4, and 8 nm) have been predicted. These gain spectra have been simulated for carrier density of  $2 \times 10^{18} / \text{cm}^3$ , and at temperature  $\sim 300\text{K}$ . In Figure 8, it can be seen that the maximum gain is decreasing with increase in width of the single quantum well sandwiched in between the barriers. In addition, the maximum gain is also found to shift towards longer wavelengths with increase in well width. After studying the gain spectra in terms of lasing wavelength, it is found that the nano-heterostructure having quantum well of 2 nm is more suitable because it provides lasing wavelength of 1.35  $\mu\text{m}$ . Here, it is very important to note that the lasing wavelength of 1.35  $\mu\text{m}$  is the wavelengths of low attenuation in the waveguide. Therefore, such heterostructures are useful in the optical fiber based communication systems based on nano-optoelectronics. Since, the maximum material gain has been achieved at wavelength of 1.35  $\mu\text{m}$  for minimum quantum well width (2 nm) with in TE mode; therefore, InGaAsP / InP based nano-heterostructure with 2 nm well width may be very useful in the area of nano-optoelectronics. In the set picture of Figure 8, the behavior of material gain in terms of photonic energy has been predicted. The behavior of well width dependent modal gain with current density has been plotted in Figure 9. From Figure 9, it may be noticed that the modal gain is increasing with increasing current density for a particular gain well width of the heterostructure. Moreover, the gain curves are shifting

towards higher current densities with increasing well widths that represents reduction in optical gain of the structure. In addition, it also represents the enhancement in transparency current density, as shown in Figure 9. The transparency current density has played a very important role in estimating the ultimate achievable threshold current density for a specific material system [17,18]. At transparency current density, the net gain does not exist because of balancing the optical gain by background absorption internal optical loss. Moreover, the differential gain becomes maximum at transparency current density.

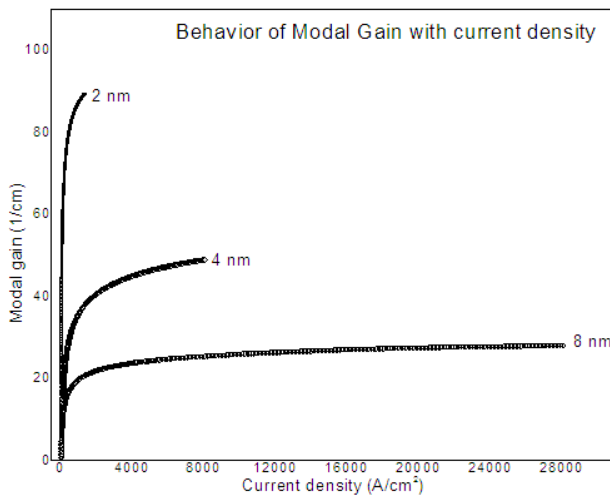


**Figure 9.** Well width dependence of modal gain of InGaAsP / InP Nano-heterostructure

## 4. Conclusion

In this paper, the effects of quantum well width on material gain and lasing wavelength of the SCH InGaAsP / InP lasing nano-heterostructure have been discussed. The studies made in this paper are directed towards the well width dependent modeling of InGaAsP / InP lasing nano-heterostructure and simulation of the lasing characteristics such as material gain, differential gain, anti-guiding factor and refractive index change with carrier density. The outcomes of the work reported in this paper suggest that both the material gain and lasing wavelength can be controlled by varying width of the quantum well sandwiched between the barriers followed by claddings in the nano-structure. Since, the maximum material gain has been achieved at wavelength of 1.35  $\mu\text{m}$  for minimum quantum well width (2 nm) with in TE mode; therefore,

InGaAsP / InP based nano-heterostructure with 2 nm well width may be very useful in the area of nano-optoelectronics.

## Acknowledgement

P. A. Alvi and F. Rahman are thankful to University Grant Commission (UGC), Government of India, New-Delhi for financial support through minor project with Ref. F. No. 42-1067 / 2013 (SR).

## References

- [1] P. A. Alvi, Sapna Gupta, M. J. Siddiqui, G. Sharma, and S. Dalela, *Physica B: Condensed Matter*, Vol. 405, pp. 2431-2435 (2010).
- [2] P. A. Alvi, Sapna Gupta, P. Vijay, G. Sharma, M. J. Siddiqui, *Physica B: Condensed Matter*, Vol. 405, pp. 3624-3629 (2010).
- [3] Wang Yang, Qiu Ying-Ping, PAN Jiao-Qing, ZHAO Ling-juan, ZHU Hong-Liang, Wang Wei, *Chin. Phys. Lett.* 27, No. 11, 114201 (2010).
- [4] M. Bugajski, B. Mroziejewicz, K. Reginski, J. Muszalski, J. Kubica, M. Zbroszczyk, P. Sajewicz, T. Piwonski, A. Jachymek, R. Rutkowski, T. Ochalski, A. Wojcik, E. Kowalczyk, A. Malag, A. Kozłowska, L. Dobrzanski, and A. Jagoda, *Opto-Electronics Review* 9 (1) (2001).
- [5] Durga Prasad Sapkota, Madhu Sudan Kayastha, Kiochi Wakita, *Opt. Quant Electron.*, 45 35-43 (2013).
- [6] Carsten Rohr, Paul Abbott, Ian Ballard, James P. Connolly, and Keith W. J. Barnham, Massimo Mazzer, Chris Button, Lucia Nasi, Geoff Hill and John S. Roberts, Graham Clarke, Ravin Ginige, *J. of Appl. Phys.*, 100, 114510 (2006).
- [7] L.P. Hou, M. Haji, C. Li, B.C. Qiu, and A.C. Bryce, *Laser Phys. Lett.* 8, 535 (2011).
- [8] Vahid Bahrami Yekta and Hassan Kaatuzian, *Commun. Theor. Phys.* 54, pp. 529-535 (2010).
- [9] Jong-Jae KIM, *J. of the Korean Physical Society*, 48, No. 1, pp. 166-169 (2006).
- [10] Pyare Lal, Shobhna Dixit, S. Dalela, F. Rahman, P. A. Alvi, *Physica E* 46, pp. 224-231(2012).
- [11] Beatrice Saint-Cricq, Françoise Lozes-Dupuy, and Georges Vassilieff, *IEEE J. of Quantum Electronics* QE-22, No. 5 (1986).
- [12] Sandra R. Selmic, Tso-Min Chou, Jieping Sih, Jay B. Kirk, Art Mantie, Jerome K. Butler, Gary A. Evans, *IEEE J. On Selected Topics in Quantum Electronics*, 7, No. 2 (2001).
- [13] G. D. Mahan, L. E. Oliveira, *Phys. Rev. B* 44, 3150-3156 (1991).
- [14] P. A. Alvi, Pyare Lal, S. Dalela, and M. J. Siddiqui, *Physica Scripta* 85, 035402 (2012).
- [15] Pyare Lal, Rashmi Yadav, F. Rahman, P. A. Alvi, *Adv. Sci. Eng. Med.* 5, 918-925 (2013).
- [16] N. Choudhary, N. K. Dutta, *J. Appl. Phys.*, Vol. 90, No. 1, pp. 38-42 (2001).
- [17] P. L. Derry, A. Yariv, K.Y. Lau, N. Bar-Chaim, K. Lee, J. Rosenberg, *Appl. Phys. Lett.* 50, 1773 (1987).
- [18] A. Yariv, *Appl. Phys. Lett.* 53, 1033 (1988).